Multi-Dimensional Effects in Longwave Radiative Forcing of PBL Clouds

D. B. Mechem and Y. L. Kogan
Cooperative Institute for Mesoscale Meteorological Studies
University of Oklahoma
Norman, Oklahoma

M. Ovtchinnikov
Pacific Northwest National Laboratory
Richland, Washington

K. F. Evans
University of Colorado
Boulder, Colorado

A. B. Davis
Los Alamos National Laboratory
Los Alamos, New Mexico

R. F. Cahalan
National Aeronautic and Space Administration
Goddard Space Flight Center
Greenbelt, Maryland

E. E. Takara and R. G. Ellingson
Florida State University
Tallahassee, Florida

1. Introduction

Numerical cloud models nearly universally employ one-dimensional (1D) treatments of radiative transfer (RT). Radiative transfer is typically implemented as a 2- or 4-stream approximation to the explicit RT equation. One-dimensional RT (1DRT) is computationally attractive relative to Monte Carlo methods or solving the full radiative transfer equation explicitly. However, 1DRT neglects horizontal photon transport, which may be important for situations of complex cloud geometry and internal cloud structure. The intercomparison of three-dimensional radiation codes (I3RC) project has demonstrated that 1DRT sometimes introduces systematic bias that can lead to significant errors in domain-average shortwave heating rates.

Recent studies (e.g., Zuidema and Evans 1998, Di Giuseppe and Tompkins 2003) have explored the multi-dimensional (MD) effect on albedo for boundary layer stratocumulus cloud fields. These studies typically calculate MD and independent pixel approximation (IPA, effectively 1D) radiative transfer and obtain estimates of the plane-parallel albedo bias (Cahalan et al. 1994), which is an important parameter in computing the shortwave radiation budget for the global energy balance. The MD-IPA bias is generally related to the degree of heterogeneity in the cloud field, with broken cloud systems exhibiting greater bias than solid cloud fields.

These previous studies are mainly concerned with how the cloud spatial structure modulates the radiative characteristics of a cloud system and do not address the direct influence of MD effects on cloud dynamics. For example, how does using a full MD radiative forcing relative to 1D forcing affect cloud system evolution as measured by such quantities as buoyancy flux or entrainment? Guan et al. (1995) demonstrate that longwave MDRT can produce different stratocumulus cloud top cooling rates depending on whether the cloud top is flat or undulating. Their results suggest an interactive feedback between MDRT and cloud dynamics, though their experimental framework is not able to address the ultimate effect of such a feedback. Guan et al. (1997) show that longwave cooling on the sides of a small, slab-symmetric cumulus strengthens the cumulus downdraft and promotes new development near cloud base. Guan et al. include MDRT effects in their simulation but do not isolate the forcing arising from horizontal photon flow from the total radiative forcing.

Applying incorrect radiative forcing, either in magnitude or in distribution, has the potential to bias cloud system evolution. Boundary layer stratocumulus are the most obvious example of a cloud system predominantly driven by radiative processes, namely longwave cooling at cloud top. At first glance, 1DRT seems reasonable for clouds like stratocumulus that are to a great extent horizontally uniform. However, undulations in cloud top can result in radiative forcing different from the horizontally uniform value that 1DRT produces. Furthermore, the MD effect on the forcing becomes more pronounced as the cloud fraction decreases.

We apply the multi-dimensional radiative transfer scheme of Evans (1998; Spherical Harmonics Discrete Ordinate Method [SHDOM]) to cloud fields produced by large-eddy simulation (LES) in order to produce longwave MD and 1D fluxes and heating rates. The heating rate difference field (HR_{MD} – HR_{IPA}) is analyzed in the context of LES dynamic fields in order to infer feedbacks onto the cloud-topped boundary layer dynamics and cloud field structure relative to the 1D forcing ("snapshot" comparisons). A similar analysis is performed using idealized cloud fields. Next, we couple SHDOM to a LES model to address the interactive and evolutionary behavior of the MD-1D bias and to quantify its importance. Fully interactive MD radiative transport enables us to evaluate the effect horizontal photon transport has on cloud system dynamics and evolution.

2. Methodology

The Cooperative Institute for Mesoscale Meteorological Studies (CIMMS) LES (Kogan et al. 1995, Khairoutdinov and Kogan 1999) supplies the cloud field liquid water content (LWC) data for the RT calculation. Cloud optical properties first are calculated, and then SHDOM uses a correlated k-distribution to compute longwave RT in 12 bands from 4 μm to 100 μm. SHDOM accounts for emission, absorption, and scattering of longwave radiation. Initial conditions for the LES are derived from the ASTEX A209 case simulated by Khairoutdinov and Kogan (1999). The initial CCN concentration exerts a strong influence on the ultimate cloud fraction. The unbroken cloud field in Section 3 corresponds to a heavy aerosol load, while the interactive case in Section 5 simulates a relatively low aerosol concentration in order to induce cloud breakup and enhance the MD effects. The LES is configured in a two dimensional geometry (1000 × 126 points) with 10 m grid spacing both in the horizontal and vertical. Radiative transfer calculations are also made for idealized rectangular and adiabatic liquid water content clouds (LWC). The idealized clouds have a constant width and depth, but cloud fraction is varied by changing the spacing between clouds.

For the interactive simulations, SHDOM periodically calculates the radiative forcing, which the LES then applies. Two interactive simulations are compared: one with the heating rates calculated using full MDRT, and one that subtracts the horizontal flux convergence, the cooling rates associated with horizontal photon transport. The IPA (1D) heating rate is thus related to the MD heating rate by

$$HR_{IPA} = HR_{MD} - \left(-\frac{1}{\rho c_p}\frac{\partial F_x}{\partial x}\right)$$

The grid geometry for the interactive case is 500 × 51 points, with 100 m grid spacing in the horizontal and 25 m in the vertical.

3. Snapshot Calculations from Simulated Stratocumulus

Figure 1 shows that for an unbroken cloud the differences between MD and IPA heating rates are most prominent near cloud top undulations. Regions of high cloud tops are generally associated anomalous cooling ($HR_{MD} - HR_{IPA} < 0$), while low cloud tops are associated with anomalous warming ($HR_{MD} - HR_{IPA} > 0$). The shape of the undulating cloud top is largely dictated by the eddy structure, with billows (high cloud tops) associated with updrafts and valleys (low cloud tops) with downdrafts. Probability distribution functions (PDFs) corresponding to the regions of anomalous heating and cooling rates are shown in Figure 2. The PDFs illustrate that the occurrence of positive and negative regions of $HR_{MD} - HR_{IPA}$ are very nearly equal. It is thus not surprising that the vertical profile of mean $HR_{MD} - HR_{IPA}$ is very nearly zero (not shown).

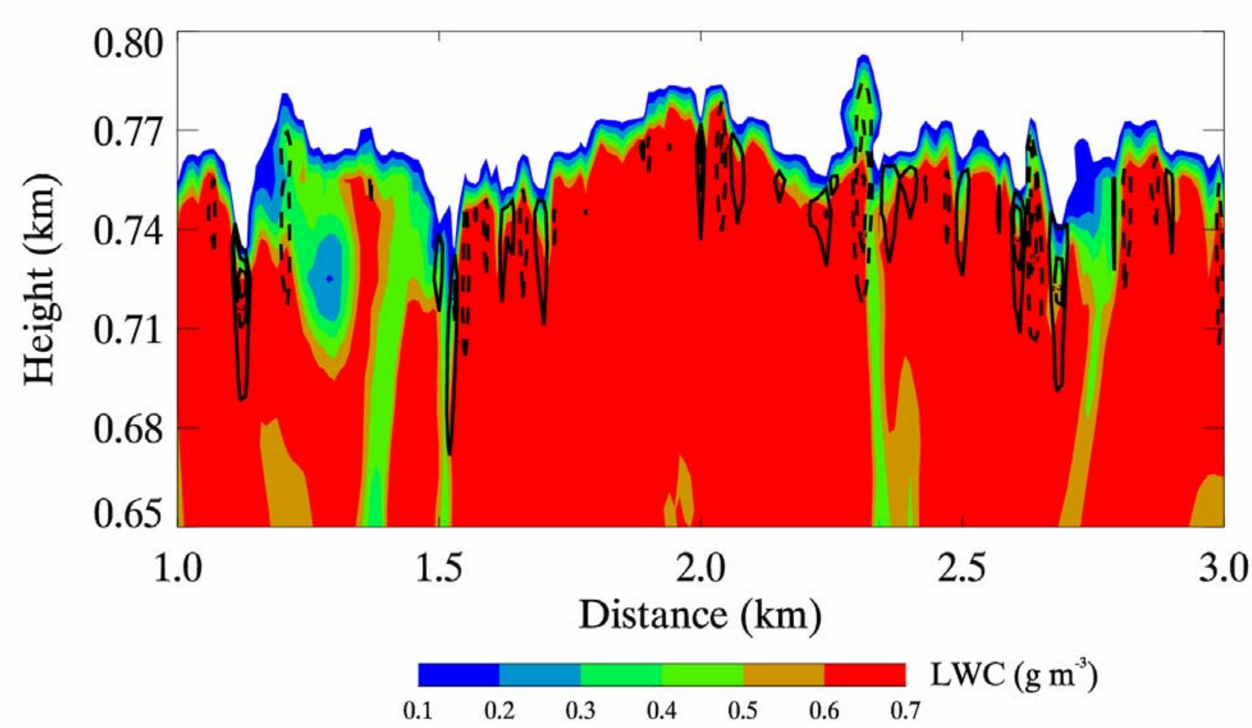

Figure 1. Vertical cross section of LWC (g m^{-3}) over the upper portion of the cloud for a subset of the calculation domain. Contours of $HR_{MD} - HR_{IPA}$ (1.0 K h$_{-1}$ interval are superimposed.

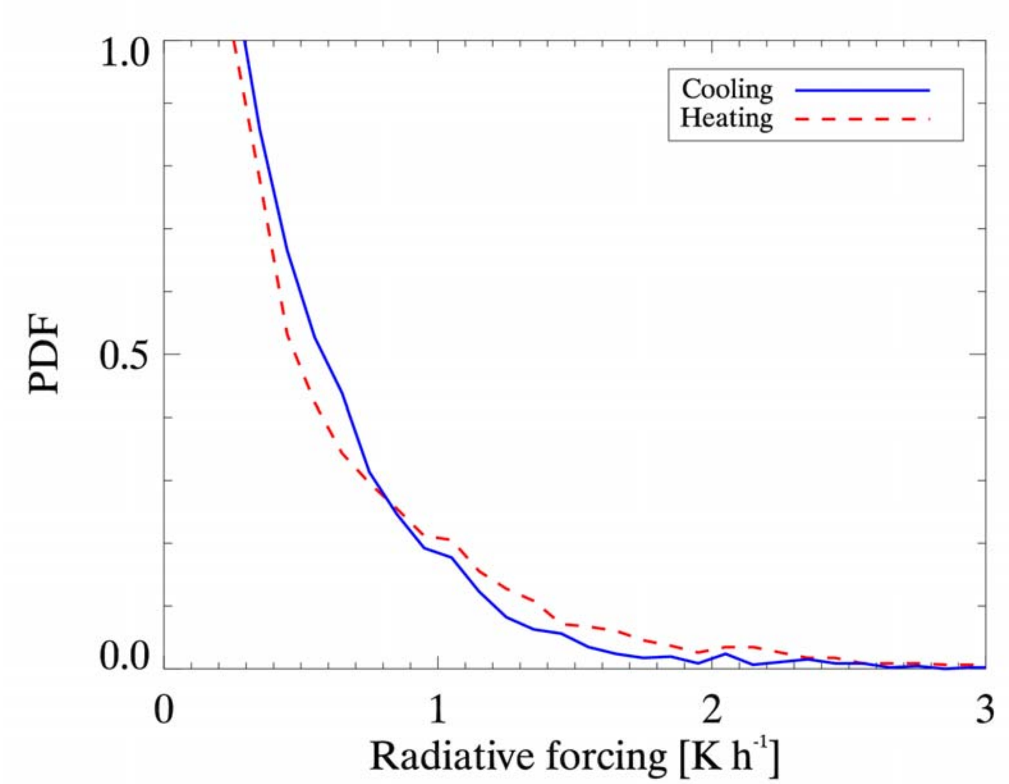

Figure 2. PDFs of positive and negative regions of $HR_{MD} - HR_{IPA}$. In order that the PDF correspond directly to energetic units, the PDFs are expressed as a function of flux convergences normalized to a heating rate by a constant density.

Since the mean radiative forcing is quite small because of the canceling effect of positive and negative anomalies, we might be tempted to conclude that any MD effect would be insignificant. However, the regions of anomalous cooling are generally associated with cloud top billows that are typically associated with updrafts. Similarly, anomalous warming is present in cloud top valleys, which are normally in downdraft regions. For this reason, the covariance,

$$\overline{w'\left(\left.\frac{dT}{dt}\right|_{MD} - \left.\frac{dT}{dt}\right|_{IPA}\right)}$$

tends to be mostly negative in the upper region of the cloud, as seen in Figure 3 and confirmed by the mean profile in Figure 4. Figure 3 also contains regions of positive covariance that arise because of multiple scales of variation in the cloud top structure. The cloud top variability scale that most closely matches the boundary layer eddy structures tends to be reliably associated with negative values of covariance. Although the covariance does not correspond rigorously to any term in the governing equations, notions of thermal buoyancy dictate that this negative correlation might tend to damp the PBL energetics.

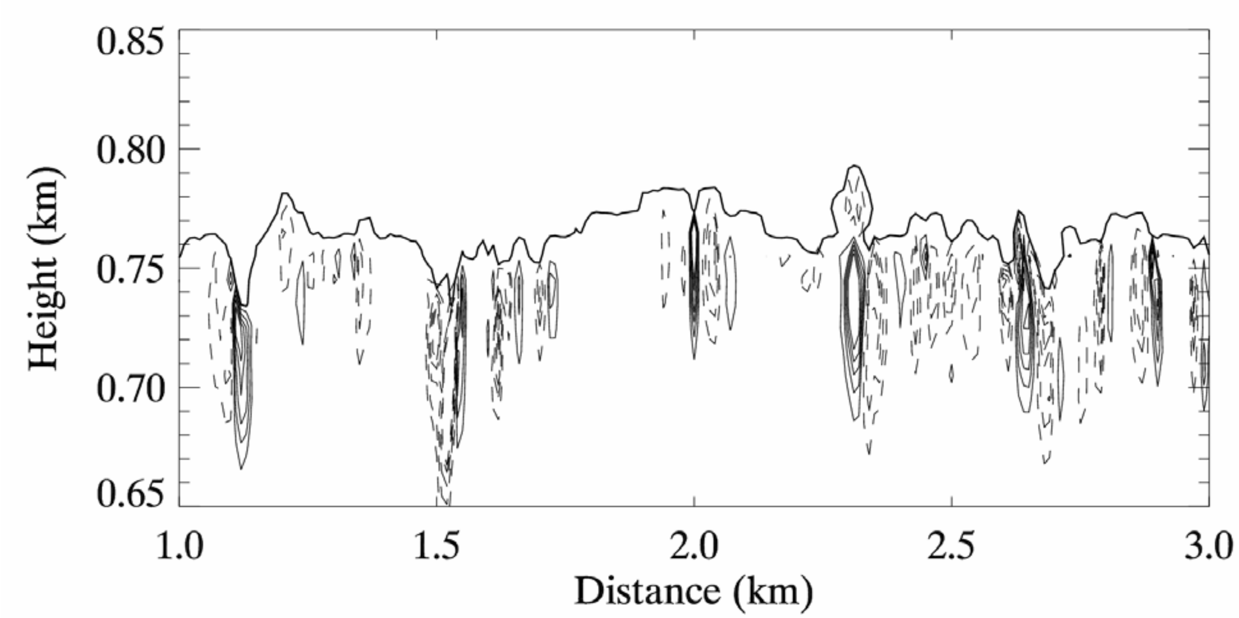

Figure 3. Vertical cross section of mean covariance of vertical velocity and $HR_{MD} - HR_{IPA}$. The contour interval is 3×10^{-5} m K s^{-2}.

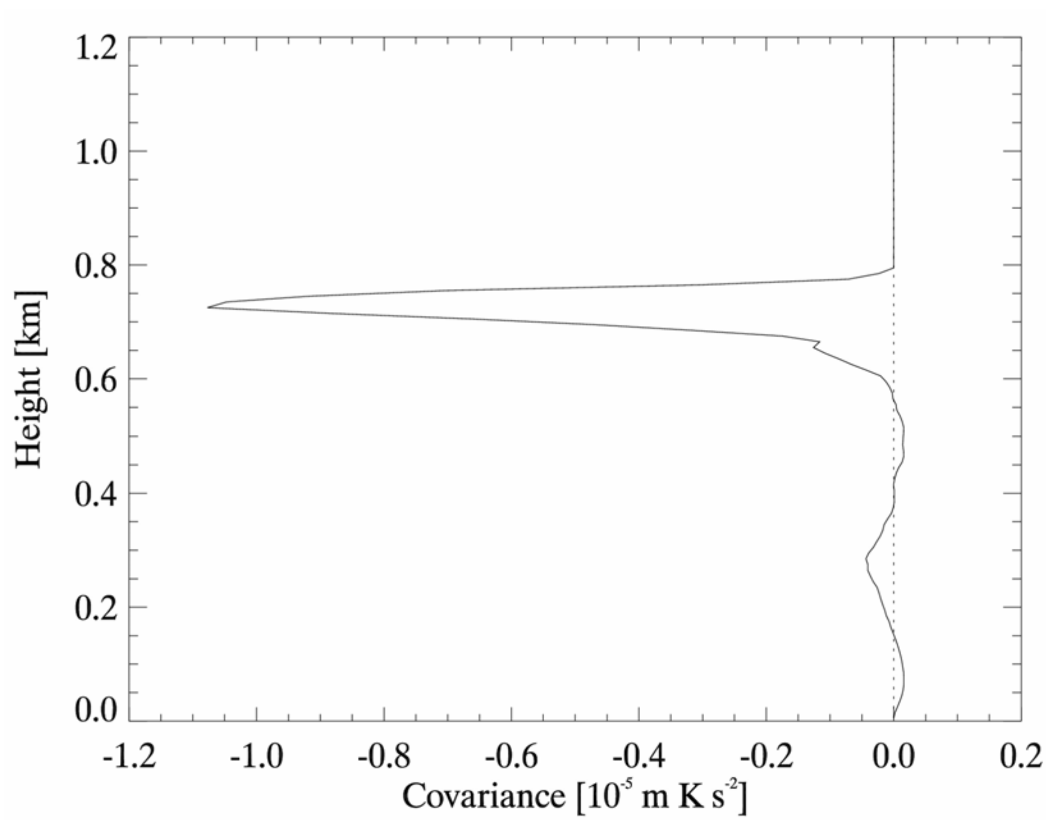

Figure 4. Vertical profiles of mean covariance of vertical velocity and $HR_{MD} - HR_{IPA}$.

4. Snapshot Calculations of Idealized Cloud Structures

To explore the contribution of the horizontal radiative fluxes relative to the total, MD and IPA radiative transfer calculations were performed for idealized rectangular clouds. Figure 5 shows an example of these rectangular cloud structures. Cloud elements are 200 m wide and 400 m deep, with a cloud base 400 m above the surface. LWC is a constant 0.5 g m^{-3}. Calculations were also performed for an adiabatic cloud representative of a mixed layer, which varies linearly over the cloud layer from 0 to 0.5 g m^{-3}. Cloud fraction is varied by changing the spacing between clouds. The spacing in between clouds in Figure 5 is 200 m, giving a cloud fraction of 0.5.

The $HR_{MD} – HR_{IPA}$ pattern in Figure 6 illustrates the lateral cooling of the rectangular cloud elements. As expected, cooling tends to be greater over the upper part of the cloud boundary, though it becomes more evenly distributed as the cloud fraction decreases. Figure 7 shows the relative contribution to the total fluxes of the horizontal component, calculated as energetic contributions (i.e., W m^{-3}). The horizontal contribution increases with decreasing cloud fraction down to ~0.25. These calculations for Figures 5 and 6 were performed with constant LWC; however, Figure 7 shows that assuming adiabatic cloud structure changes the relative contribution very little. Although the lateral cooling rates are less than ½ of the cloud top cooling rate, the lateral cloud area is double that of the cloud top area, making for a significant contribution to the total cloud forcing.

5. Interactive MDRT and IPA Simulations

In the fully interactive simulations, the longwave MD effect is realized via the manner in which the MD heating rates modify the thermal buoyancy field relative to the 1D RT solution. This mechanism is the direct radiative-dynamic feedback of interest. The LES is run for an hour using its own two-stream RT scheme to establish a reasonable boundary layer structure. Then, two simulations are conducted using the MD and IPA heating rates from SHDOM, as described in Section 2. Because of computational expense, the RT calculation is performed every 10 timesteps. Relative to calculating RT every timestep, we estimate that calculating every 10 timesteps introduces an RMS error of ~3% in heating rates.

Differences in statistics (not shown) between MD and IPA experiments develop but do not appear to exhibit any systematic bias in this relatively short simulation (5 h). Furthermore, as the cloud field breaks apart, the limited number of drizzle cells (realizations) in the domain introduces significant noise in the evolution statistics. The vertical profile of cloud fraction at hourly intervals in Figure 8 also shows little change between MD and IPA simulations. The slight reduction of cloud fraction in the IPA simulation at 6 h seems opposite to the sense the MD cooling rates would imply, since the cloud top lateral cooling should enhance the negative buoyancy there and enhance cloud breakup. In any case, the difference between MD and IPA cloud fractions are of the same magnitude as the cloud fraction from different LES realizations.

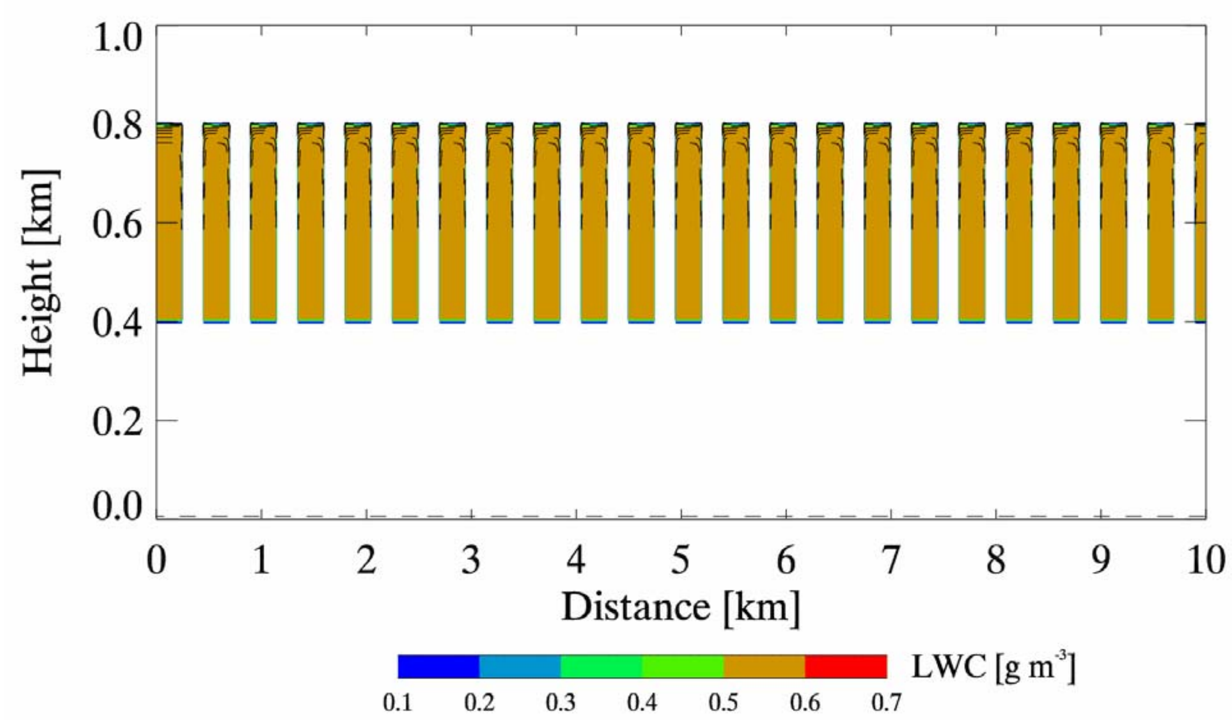

Figure 5. LWC and MD heating rate (contour interval of 2.5 K h^{-1}) for idealized rectangular clouds.

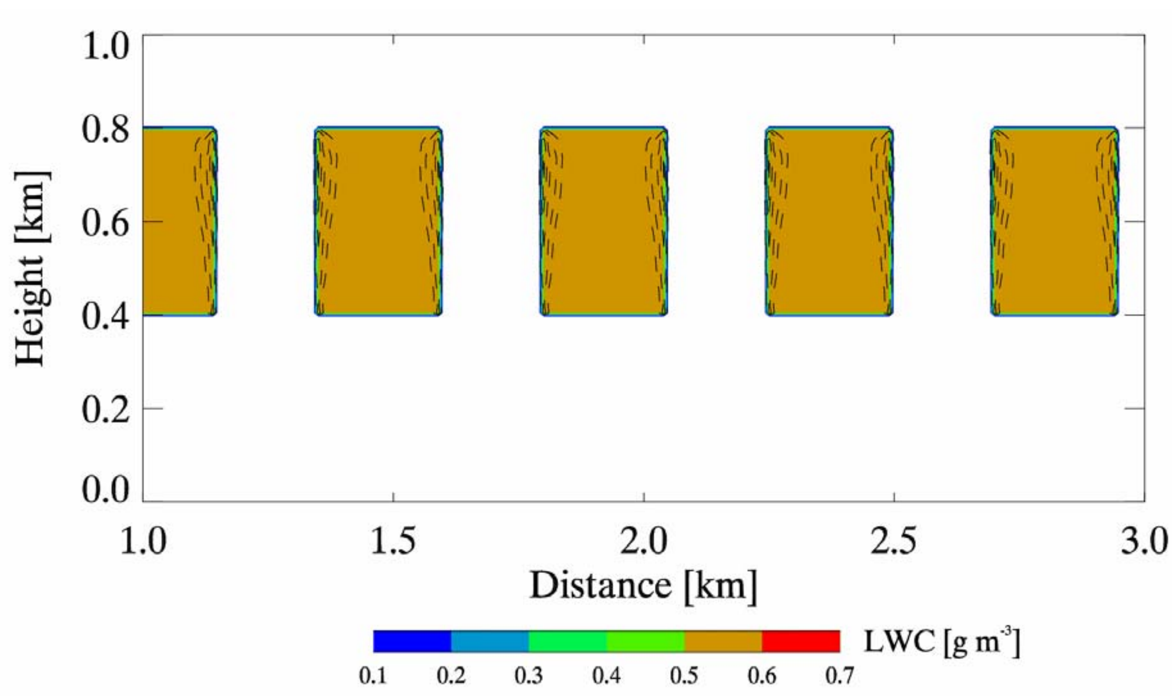

Figure 6. LWC and $HR_{MD} - HR_{IPA}$ heating rate anomaly (contour interval of 1.0 K h^{-1}, zero contour omitted).

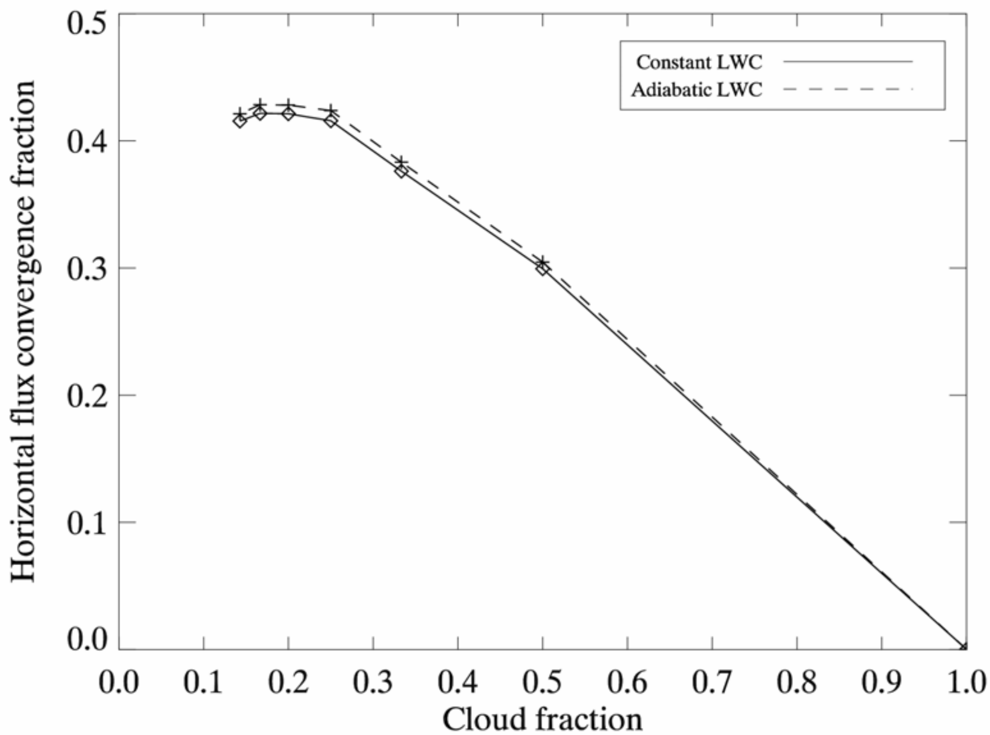

Figure 7. Relative contribution to the total radiative fluxes of the horizontal component as a function of cloud fraction.

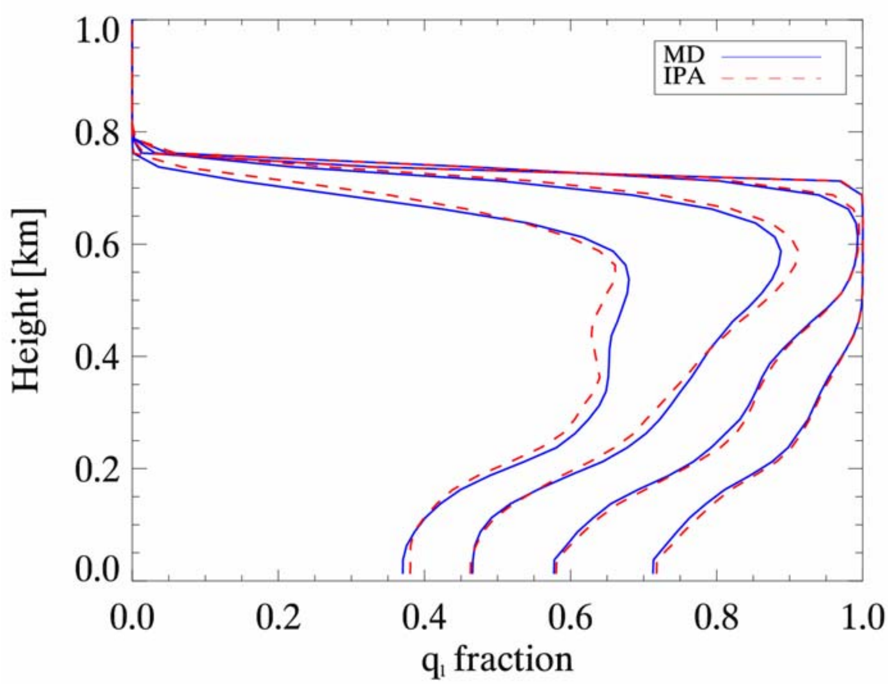

Figure 8. Hourly mean cloud fraction profiles for MDRT and IPA simulations.

6. Discussion

The snapshot calculations demonstrate a strong negative correlation between longwave HR_{MD} – HR_{IPA} forcing anomalies and eddy structure that for an unbroken LES cloud field implies a negative feedback on PBL energetics. Although not shown, drastic differences in the evolution of specific cloud and eddy structures between the MD and IPA simulations are visible. This is to be expected, since small perturbations in a turbulent flow can have a dramatic impact on the final solution. However, despite a strong correlation between MD-IPA heating rate anomalies and eddies that implies a negative feedback on the boundary layer energetics, statistics for the interactive simulations show little difference between the MD and IPA simulations. This result indicates that the typical 1D, plane-parallel methods of radiative transfer nearly universally applied in numerical models may be sufficiently accurate for longwave forcing of cloud topped boundary layer dynamics.

> Why then do statistics for our interactive MD and IPA simulations show so little systematic bias?

We have two current working hypotheses. First, during the early phase characterized by large cloud fraction, the horizontal flux convergence may be only a minor contribution to the total forcing; in other words, the overall forcing from the vertical flux convergence is much greater than forcing from the lateral cooling. Second, the low cloud fraction regime exhibits a prominent MD effect in the snapshot calculations but also tends to be associated with boundary layer decoupling and energetics that may be more surface-based and less radiatively driven. Thus, the radiative term becomes a smaller portion of the total forcing.

7. Acknowledgements

This research was supported by the Environmental Sciences Division of the U. S. Department of Energy (through Battelle PNR Contract 144880-A-Q1 to the Cooperative Institute for Mesoscale Meteorological Studies) as part of the Atmospheric Radiation Measurement Program, and by ONR N00014-96-1-0687 and N00014-03-1-0304.

8. Corresponding Author

D. B. Mechem, dmechem@ou.edu, 405-325-6103

9. References

Cahalan, R. F., W. Ridgeway, W. J. Wiscombe, and T. L. Bell, 1994: The albedo of fractal stratocumulus clouds. *J. Atmos. Sci.*, **51**, 2434–2455.

Di Giuseppe, F., and A. M. Tompkins, 2003: Effect of spatial organization on solar radiative transfer in three-dimensional idealized stratocumulus cloud fields. *J. Atmos. Sci.*, **60**, 1774–1794.

Evans, K. F., 1998: The spherical harmonics discrete ordinate method for three-dimensional atmospheric radiative transfer. *J. Atmos. Sci*., **55**, 429–446.

Guan, H., R. Davies, and M. K. Yau, 1995: Longwave radiative cooling rates in axially symmetric clouds. *J. Geophys. Res*., **100**, 3213–3220.

Guan, H., M. K. Yau, and R. Davies, 1997: The effects of longwave radiation in a small cumulus cloud. *J. Atmos. Sci*., **54**, 2201–2214.